Synthesis of New ESIPT-Fluorescein: Photophysics of pH Sensitivity and Fluorescence

ARTICLE *in* THE JOURNAL OF PHYSICAL CHEMISTRY A · DECEMBER 2011

Impact Factor: 2.69 · DOI: 10.1021/jp2073123 · Source: PubMed

6 AUTHORS, INCLUDING:

Vikas S. Patil
Institute of Chemical Technology, Mumbai
46 PUBLICATIONS **230** CITATIONS
SEE PROFILE

Vikas Padalkar
Osaka University
41 PUBLICATIONS **340** CITATIONS
SEE PROFILE

Kiran Phatangare
24 PUBLICATIONS **229** CITATIONS
SEE PROFILE

Sekar Nagaiyan
Institute of Chemical Technology, Mumbai
70 PUBLICATIONS **253** CITATIONS
SEE PROFILE

THE JOURNAL OF PHYSICAL CHEMISTRY A

ARTICLE

pubs.acs.org/JPCA

Synthesis of New ESIPT-Fluorescein: Photophysics of pH Sensitivity and Fluorescence

Vikas S. Patil, Vikas S. Padalkar, Kiran R. Phatangare, Vinod D. Gupta, Prashant G. Umape, and Nagaiyan Sekar*

Institute of Chemical Technology (Formerly UDCT), N. P. Marg, Matunga, Mumbai, 400 019 Maharashtra, India

Supporting Information

ABSTRACT: ESIPT-inspired benzimidazolyl substituted fluorescein dyes were synthesized. PH-sensitivity was determined by the photophysical property measured at a physiological possible pH range. Fluorescence quantum efficiency values were calculated independently at two different emissions. A rational relationship is defined between fluorescence quantum efficiency and calculated HOMO energy.

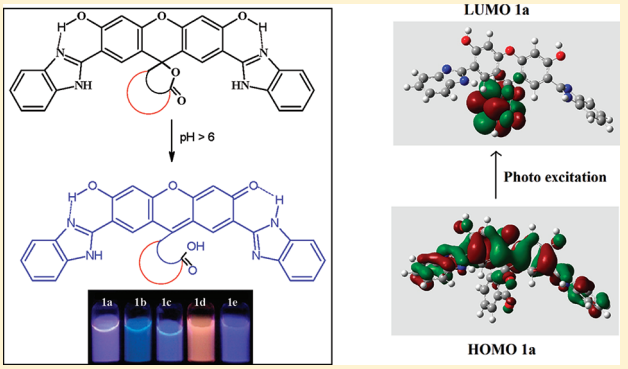

INTRODUCTION

Fluorescence probes are excellent sensors for biological pH for the reasons that they are sensitive combined with fast response. Fluorescent pH sensors find wide use in analytical chemistry, bioanalytical chemistry, cellular biology (for measuring intracellular pH), and medicine.[1−3] Among other pH measurement methods, fluorescence spectroscopy has advantages with respect to spatial and temporal observation of pH changes. They tend to be operationally simple, and they are in most cases nondestructive to cells. Development of optical pH chemosensors,[4−8] with specific requirement of highly sensitive indicators within the physiological pH range,[9,10] is currently a fertile area of research. In this area, fluorescein and its derivatives are perhaps the most widely used fluorescent pH probes[11−14] due to their excellent photophysical properties.

However, fluorescence measurements are largely influenced by many factors, including optical path length, changes of temperature, altered excitation intensities, and varied emission collection efficiencies. In order to circumvent these problems an alternative, viz., a ratiometric detection technique is used.

Ratiometric fluorescent measurements make use of changes in the ratio of the intensities of the emission at two wavelengths.[15] Thus, ratiometric fluorescent sensors have an advantage that they can be used to evaluate the analyte concentration with a provision of built-in correction for environmental effects. Ratiometric fluorescence spectroscopic methods rely heavily on fluorescent sensors that are differentially sensitive to protons for at least two excitation or emission wavelengths.[16,17] For example, for a suitable fluorescent dye, emission at one carefully chosen wavelength may be enhanced or diminished relative to the emission at another. Ratios between these signals then can be calibrated to indicate pH values. Advantages when using ratiometric methods are accrued because parameters such as optical path length, local probe concentration, photobleaching, and leakage from the cells are irrelevant. This must be so since both signals come from the probe in exactly the same environment.

Fluorescent molecules exhibiting dual emission are those exhibiting excited state intramolecular proton transfer (ESIPT). A variety of molecules have intramolecular hydrogen bonds (H-bonds) that may be photo-induced to undergo proton transfer. ESIPT can be observed in a variety of such molecules that contain both hydrogen donor and acceptor in close proximity.[18−26] An intramolecular hydrogen bond generally formed in the ground state will migrate to the neighboring proton acceptor leading to a phototautomer.[27−29] In the general family of 2-(2′-hydroxyphenyl) benzimidazole, benzoxazole, benzthiazole, and benztriazole,[30−33] the ESIPT phototautomer gives rise to an emission with large Stokes shift. The high intensity of fluorescence emission and large Stokes shift due to intramolecular proton transfer phenomena[34−48] allow these molecules to have many interesting applications. Molecules undergoing ESIPT exhibit dual fluorescence, one a normal Stokes shifted fluorescence band and another originating from a tautomer formed in the exited state. Further the fluorescence band maximum and the fluorescence quantum yield

Received: August 1, 2011
Revised: November 19, 2011
Published: December 05, 2011

Scheme 1. Synthesis of Fluorescein Derivatives (1a−1e)

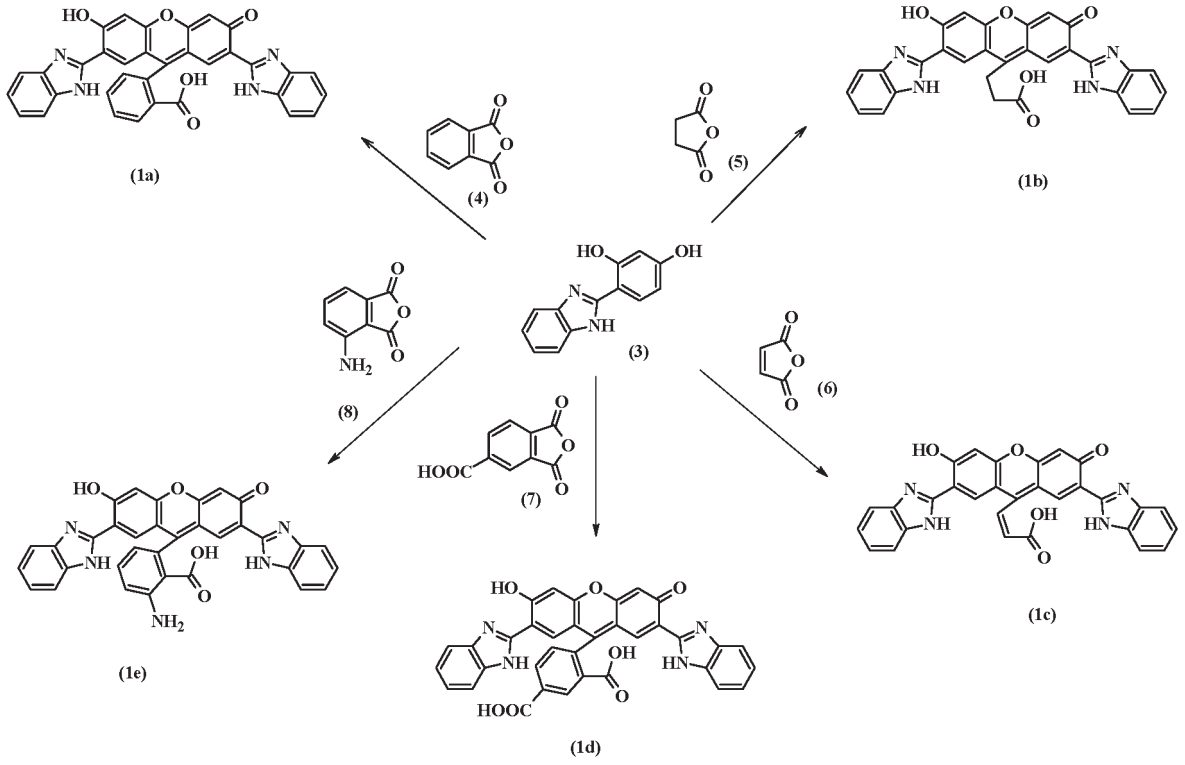

of the tautomer fluorescence band are very sensitive, whereas those of the normal band do not depend much on the environment. It is commonly understood that the molecular structure of the ESIPT compounds regulates their abnormal photophysical properties to a considerable extent, in most cases exceeding the influence of the environment on them. There is an example 2-(3,5,6-trifluoro-2-hydroxy-4-methoxyphenyl) benzoxazole, a fluorophore, that undergoes intramolecular hydrogen bonding.[49]

The molecules showing ESIPT particularly *o*-hydroxy benzazoles have absorption in the UV region and emission in the visible region. An attempt has been made in this work to incorporate an ESIPT unit in a molecule having absorption in the visible region.

EXPERIMENTAL SECTION

Materials and Equipment. All commercial reagents and solvents were procured from S.D. Fine Chemicals (India) and were used without purification. The reaction was monitored by TLC using 0.25 mm E-Merck silica gel 60 F254 precoated plates, which were visualized with UV light. Melting points were measured on a standard melting point apparatus from Sunder Industrial Product, Mumbai, and are uncorrected. The FT-IR spectra were recorded on a Perkins-Elmer 257 spectrometer using KBr discs. ^{1}H NMR and ^{13}C NMR spectra were recorded on a VXR 300-MHz instrument using TMS as an internal standard. Mass spectra were recorded on Lcq Advantage Max Thermo Electron Corporation by negative mode analysis. The visible absorption spectra of the compounds were recorded on a Spectronic Genesys 2 UV−visible spectrophotometer and UV−visible emission spectra were recorded on JASCO−FP 1520 and Cary Eclipse fluorescence spectrophotometer (Varian, Australia). Simultaneous DSC-TGA measurements were performed on simultaneous DSC-TGA Waters (India) Pvt. Ltd.

SYNTHESIS AND CHARACTERIZATION

Synthesis of 4-(1*H*-Benzo[*d*]imidazol-2-yl) Benzene-1,3-diol (3). 2,4-Dihydroxy benzoic acid **1** (10 g, 64.9 mmol), and *o*-phenylenediamine **2** (7.012 g, 64.9 mmol) were mixed in polyphosphoric acid (121.94 g). The mixture was stirred at 250 °C for 4 h, and then it was allowed to cool at room temperature and poured into 1200 mL of ice-cold water with constant stirring. A dark brown precipitate was obtained, which was filtered and dissolved in a cold solution of 10% Na_2CO_3 (15.75 g dissolved in 137 mL of water) acidified with 1:1 HCl (40 mL) at 10 °C. This solution was kept overnight at 0 °C to give the final product. Yield: 55%. Melting point = >300 °C. Mass: *m*/*z* 226 (M+). ^{1}H NMR ($(CD_3)_2SO$, 300 MHz): δ 6.88 (d, 1H, 6.4 Hz), 6.88 (d, 1H, 6.4 Hz), 7.05 (s, 1H), 7.34 (s, 2H), 7.71 (s, 2H), 8.07 (s, 1H), 11.2 (s, 1H) ppm. FT-IR (KBr, cm^{-1}): 3438 (phenolic O−H), 3322 (N−H), 1651 (imine C═N), 1571 (aromatic C═C), 1516, 1421, 1389, 1203 (phenol C−O).

General Procedure for the Synthesis of Fluorescein Derivatives (1a−1e). 4-(1*H*-Benzo[*d*]imidazol-2-yl) benzene-1,3-diol **3** (88 mmol) was mixed with different anhydrides (**4**−**8**) (44 mmol) in H_2SO_4 and heated at 160 °C for 4 h and was allowed to cool at room temperature. The reaction mixture was poured into 100 mL ice-cold water and stirred for 15 min. The precipitated product was filtered and washed with cold water (25 mL).

Purification of Fluorescein Derivatives (1a−1e). The crude product was purified by dissolving it into 10% Na_2CO_3 solution (46 mL) and acidified with 1:1 HCl (13 mL) to give the final compounds (**1a**−**1e**).

dx.doi.org/10.1021/jp2073123 |*J. Phys. Chem. A* 2012, 116, 536–545

Table 1. UV−Vis Absorption and Fluorescence Maxima Data of Dyes 1a−1e from pH 6 to 13 at 1×10^{-6} mol L^{-1}

	1a			1b			1c			1d			1e		
pH	absorption	emission	Δλ	absorption	emission	Δλ	absorption	emission	Δλ	absorption	emission	Δλ	absorption	emission	Δλ
6	303(0.54)	408(1.68)	105	300(0.39)	436(1.05)	136	294(1.08)	462(0.75)	168	285(0.27)	436(82.98)	151	300(0.12)	425(730.24)	125
		568(0.79)	265				489(0.41)				570(68.11)	285	545(0.37)		
	432(0.46)									495(0.25)					
	543(0.36)														
7	303(0.57)	434(1.50)	131	300(0.43)	440(1.00)	140	318(0.50)	462(0.73)	144	285(0.27)	435(66.99)	152	300(0.18)	430(581.61)	130
		570(0.56)	267				492(0.09)				572(305.65)	287	540(0.21)		
	495(0.41)									495(0.12)					
	543(0.51)														
8	303(0.55)	434(1.48)	131	300(0.42)	434(2.00)	134	318(0.47)	462(0.73)	144	300(0.25)	435(78.20)	135	300(0.27)	428(703.07)	128
		570(0.59)	267				540(0.10)				572(382.59)	272	490(0.15)		
	495(0.34)								495(0.25)				535(0.08)		
	543(0.58)														
9	303(0.55)	432(1.37)	129	300(0.43)	434(2.00)	134	297(0.047)		144	300(0.27)	435(76.74)	135	300(0.21)	425(612.67)	125
		568(0.69)	265				317(0.49)	462(0.71)			572(340.72)	272	540(0.07)		
	495(0.36))						354(0.29)			495(0.22)					
	543(0.57)						537(0.10)			545(0.20)					
10	303(0.53)	410(1.81)	107	297(0.40)	412(1.80)	115	297(0.45)			305(0.27)	436(42.58)	131	305(0.21)	405(857.51)	100
		570(1.23)	267		560(0.25)	263	342(0.50)	458(0.68)	116		570(68.89)	265	540(0.10)		
	543(0.81)			336(0.35)			540(0.16)			500(0.19)					
				354(0.33)						545(0.24)					
				540(0.09)											
11	303(0.51)	412(1.90)	109	300(0.40)	414(2.12)	114	303(0.42)			285(0.42)	435(116.22)	150	300(0.22)	443(118.78)	143
		570(1.00)	267		560(0.25)	260	354(0.64)	430(0.75)	74		572(468.99)	287		566(481.78)	266
	543(0.73)			351(0.39)			534(0.61)			495(0.34)			540(0.07)		
				531(0.10)						540(0.10)					
12	306(0.52)	416(1.19)	110	342(0.39)	416(2.20)	74	306(0.45)		72	285(0.42)	435(141.85)	150	285(0.25)	410(836.41)	125
		570(1.25)	264	357(0.41)			354(0.69)	426(0.78)			572(467.02)	287	490(0.13)		
	543(0.66)						528(0.15)			545(0.33)					
13	303(0.45)	414(1.60)	111	303(0.36)	416(3.25)	103	306(0.45)			285(0.42)	435(141.85)	150	300(0.21)	411(119.72)	111
		568(0.68)	265	360(0.41)			354(0.70)	426(0.65)	72		572(467.02)	287	345(0.21)		
	534(0.58)						522(0.13)			545(0.33)			540(0.15)		

dx.doi.org/10.1021/jp2073123 | J. Phys. Chem. A 2012, 116, 536–545

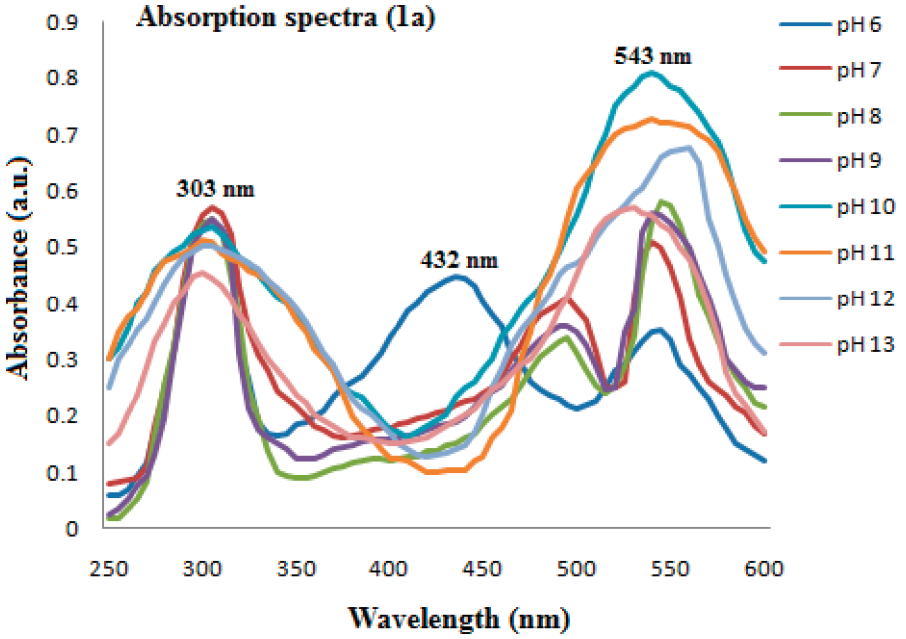

Figure 1. Absorption spectra of **1a** at various pH (6−13).

2,7′-Di(1*H*-benzo[d]imidazol-2-yl)-3′,6′-dihydroxy-3*H*-spiro-[isobenzofuran-1-9′-xanthen]-3-one (1a). Yield: 55%. Mp = >300 °C. FT-IR (KBr, cm^{-1}): 3432 (O−H), 3324 (N−H), 1768 (lactone C═O), 1740 (lactone C═O), 1689 (C═O), 1642 (C═N), 1578 (aromatic C═C), 1550 (aromatic), 1515, 1441, 1402, 1339 (C−N), 1252 (phenol C−O), 1190 (lactone C−O), 1130 (ether linkage). Mass *m*/*z* 564 (M+). ^{1}H NMR ($(CD_3)_2$SO, 300 MHz): δ 6.58 (s, 2H), 7.17 (d, 2H, 6.4 Hz), 7.34(d, 2H, 6.4 Hz), 7.68 (d, 2H, 6.4 Hz), 7.72 (dd, 2H, 6.4 Hz, 14.9 Hz), 8.00 (s, 2H), 8.2−8.3 (d, 4H, 8.9 Hz), 8.4 (s, 2H), 11.3 (bs, 2H) ppm. ^{13}C NMR ($(CD_3)_2$SO, 75 MHz): δ 85.46, 166.00, 106.29, 111.92, 115.21, 115.39, 124.11, 125.83, 127.29, 130.74, 141.71, 151.73, 152.48, 152.93. Elemental analysis: exptl, C = 72.25, H = 3.52, N = 9.88, O = 15.52; theor, C = 72.33, H = 3.57, N = 9.92, O = 14.17.

2′,7′-Di(1*H*-benzo[*d*]imidazol-2-yl)-3′,6′-dihydroxy-3*H*-spiro-[furan-2,9′-xanthen]-5(4*H*)-one (1b). Yield: 48%. Mp = >300 °C. FT-IR (KBr, cm^{-1}): 3312 (phenolic O−H), 2963(aliphatic C−H), 2924 (aliphatic C−H), 1768 (lactone C═O), 1689 (C═O), 1642 (C═N), 1578 (aromatic C═C), 1515, 1441, 1402, 1339 (C−N), 1252 (phenol C−O), 1190 (lactone C−O), 1005. Mass *m*/*z* 514 (M+). ^{1}H NMR ($(CD_3)_2$SO, 300 MHz): δ 2.47 (t, 2H), 3.57 (t, 2H), 7.71 (d, 2H, 9.2 Hz), 7.74 (dd, 2H, 9.2 Hz, 14.6 Hz), 7.78 (s, 2H), 7.99 (s, 2H), 8.02 (s, 2H), 8.33 (m, 2H, 9.2 Hz, 17.4 Hz), 8.37 (m, 2H, 9.2 Hz) ppm. ^{13}C NMR ($(CD_3)_2$SO, 75 MHz): δ 40.32, 38.66, 101.98, 103.33, 110.97, 113.13, 123.61, 129.02, 130.33, 131.02 145.78, 147.37, 159.47. Elemental analysis: exptl, C = 69.75, H = 3.82, N = 10.78, O = 15.48; theorl, C = 69.76, H = 3.90, N = 10.85, O = 15.49.

2′,7′-Di(1*H*-benzo[*d*]imidazol-2-yl)-3′,6′-dihydroxy-3*H*-spiro-[furan-2,9′-xanthen]-5-one (1c). Yield: 41%. Mp =240−242 °C. FT-IR (KBr, cm^{-1}): 3310 (phenolic O−H), 2851 (aliphatic C−H), 1734 (lactone C═O), 1696 (C═O), 1648 (C═N), 1598 (aromatic C═C), 1501, 1431, 1406, 1342 (C−N), 1252 (phenol C−O), 1192 (lactone C−O), 1018. Mass *m*/*z* 516 (M+). ^{1}H NMR ($(CD_3)_2$SO, 300 MHz): δ 6.55 (s, 2H), 7.69 (d, 2H, 8.3 Hz), 7.71 (dd, 2H, 8.3 and 10.5 Hz), 7.74 (d, 2H, 10.5 Hz), 7.76 (d, 2H, 10.5 Hz), 7.99 (s, 2H), 8.01 (s, 2H), 8.33 (s, 2H), 11.2 (s, 2H) ppm. ^{13}C NMR ($(CD_3)_2$SO, 75 MHz): δ 101.98, 103.33, 110.97, 113.13, 123.61, 125.61, 129.02, 130.33, 131.02 145.78, 147.37, 159.47, 159.57. Elemental analysis: exptl, C = 70.25, H = 3.52, N = 10.80, O = 15.52; theor, C = 70.03, H = 3.59, N = 10.89, O = 15.55

2′,7′-Di(1*H*-benzo[*d*]imidazol-2-yl)-3′,6′-dihydroxy-3-oxo-3*H*-spiro[isobenzofuran-1-9′-xanthen]-5-carboxylic acid (1d). Yield: 57%. Mp = > 300 °C. FT-IR (KBr, cm^{-1}): 3277 (phenolic O−H), 3210, 1759 (lactone C−O), 1731 (C═O), 1700 (C═O), 1667 (C═N), 1627, 1588 (aromatic C═C), 1496, 1404, 1337 (C−N), 1317, 1261, 1180 (lactone C−O), 1124 (lactone C−O), 1060, 841, 805, 755, 668. Mass *m*/*z* 608 (M+). ^{1}H NMR ($(CD_3)_2$SO, 300 MHz): δ 6.00 (s, 1H), 7.15 (s, 2H), 7.52 (s, 1H), 7.55 (s, 1H), 7.66 (m, 8H, 10.0 Hz, 8.8 Hz), 7.02 (m, 2H, 11.4 Hz, 8.8 Hz), 7.84 (d, 1H, 11.4 Hz), 7.94 (d, 2H, 8.8 Hz), 8.34 (s, 1H), 8.60 (s, 1H) ppm. ^{13}C NMR ($(CD_3)_2$SO, 75 MHz): δ 80.99, 104.24, 108.35, 111.16, 111.46, 113.35, 123.45, 126.31, 129.98, 131.51, 132.19, 133.17, 145.50, 147.32, 153.50, 156.08, 159.40, 166.22, 168.13. Elemental analysis: exptl, C = 69.15, H = 3.32, N = 9.18, O = 18.32; theor, C = 69.08, H = 3.31, N = 9.21, O = 18.40.

4-Amino-2′,7′-di(1*H*-benzo[*d*]imidazole-2-yl)-3′,6′-dihydroxy-3*H*-spiro-[isobenzofuran-1-9′-xanthen]-3-one (1e). Yield: 51%. Mp = >300 °C. Mass *m*/*z* 579 (M+). FT-IR (KBr, cm^{-1}): 3445, 1734 (ester C═O), 1700 (C═O), 1650 (C═O), 1558 (aromatic C═C), 1541, 1490, 1457, 1398, 1342 (C−N), 1258 (phenol C−O), 1177 (ester C−O), 1104 (ester C−O), 1048, 869, 822, 668. ^{1}H NMR ($(CD_3)_2$SO, 300 MHz): δ 5.99 (s, 2H), 6.58 (s, 2H), 6.97 (s, 2H), 7.12 (s, 2H), 7.75 (m, 8H, 11.9 Hz, 14.2 Hz), 8.02 (m, 3H, 12.4 Hz, 11.9 Hz), 8.34 (s, 2H). ^{13}C NMR ($(CD_3)_2$SO, 75 MHz): δ 99.22, 101.52, 109.27, 111.37, 121.89, 123.44, 127.21, 128.61, 129.24, 145.58, 157.62, 157.75. Elemental analysis: exptl, C = 70.38, H = 3.62, N = 12.01, O = 13.72; theor, C = 70.46, H = 3.65, N = 12.08, O = 13.80.

Preparation of Working Solutions for Photophysical Measurements. All the solutions were freshly prepared in water (pH was maintained by 10% NaOH and 1:1 HCl) before recording

dx.doi.org/10.1021/jp2073123 |*J. Phys. Chem. A* 2012, 116, 536–545

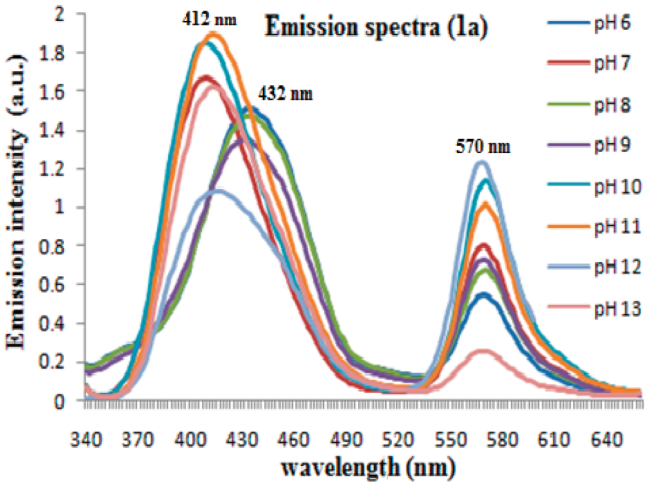

Figure 2. Fluorescence spectra of **1a** at various pH (6−13).

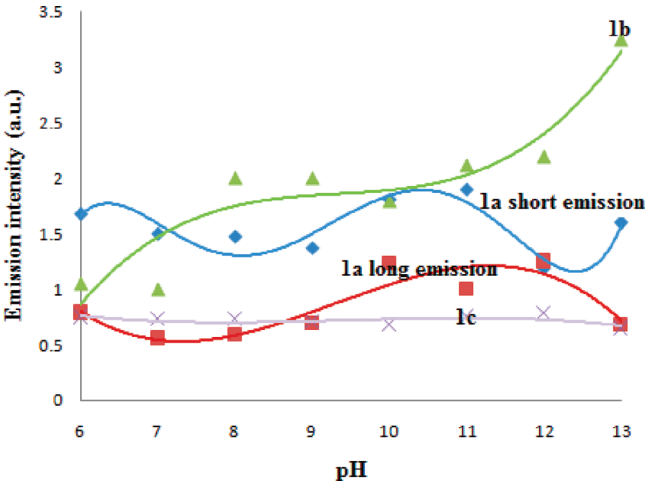

Figure 3. Fluorescence intensity against pH (compounds **1a**, **1b**, and **1c**).

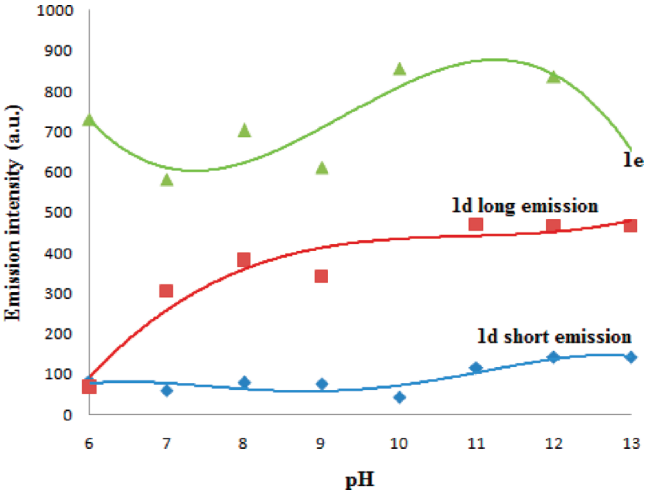

Figure 4. Fluorescence intensity against pH (compounds **1d** and **1e**).

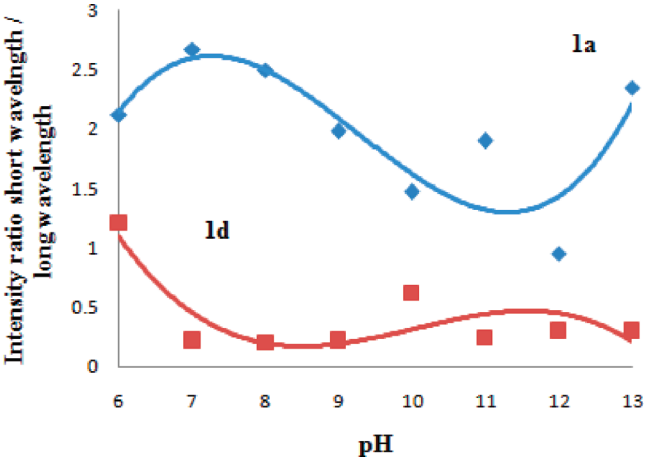

Figure 5. Ratiometry of dual emission vs pH.

the absorption and emission spectra. The concentration of prepared samples was 1×10^{-6} mol L^{-1}, and the temperature during analysis was at room temperature, 28 °C. For quantum yield calculations, the sample concentration was 2 ppm to 10 ppm in the same solvent.

RESULTS AND DISCUSSION

Synthesis and Characterization of Dyes. The reaction of 2,4-dihydroxy benzoic acid **1** with *o*-phenylenediamine **2** in polyphosphoric acid at 250 °C furnished the required ESIPT moiety 4-(1*H*-benzo[*d*]imidazol-2-yl)benzene-1,3-diol **3** with good yield (Scheme 1, Supporting Information). The reaction of 4-(1*H*-benzo[*d*]imidazol-2-yl)benzene-1,3-diol **3** with phthalic anhydride **4**, succinic anhydride **5**, maleic anhydride **6**, phthalic anhydride-4-carboxylic acid **7**, and 3-amino phthalic anhydride **8** in H_2SO_4 at 160 °C for 4 h furnished the expected fluorescein derived dyes **1a**−**1e** respectively (Scheme 1).

Photophysical Properties. The fluorescein derivatives (**1a**−**1e**) contain two benzimidazole units, each adjacent to the two hydroxyl groups of the fluorescein nucleus causing an ESIPT. Unlike the known ESIPT fluorophores, these compounds (**1a**−**1e**) have a basic fluorophoric unit (that is fluorescein molecule) interacting with the ESIPT residue.

The UV−vis absorption and fluorescence emission spectra of dyes (**1a**−**1e**) at 1×10^{-6} mol L^{-1} solution in water were measured at different pH ranging from 6 to 13. Absorption and emission maxima are also reported in the Table 1. UV−visible absorption-emission spectra of these dyes with respect to pH are highly dependable.

Author: Presence of the ESIPT benzimidazole substituent in the final structure of the dye molecule was found to be more responsible for influencing the photophysical properties. In addition to the ESIPT, the distribution of electron density on the phthalein ring plays a major role in the photophysical behavior of dye molecules. When there is an electron withdrawing group present on the phenyl ring (which does not contain a benzimidazolyle residue) of the xanthene chromophore, long wavelength emission is observed. On the contrary, when electron releasing substituent is present, a blue shift is observed. Dye **1a** has an excitation at 300 nm, which was totally unaffected by the pH. It was observed that in the case of dye **1a** in addition to the usual excitation at 495 nm (characteristic of fluorescein molecule), additional excitation occurred at 543 nm. It is interesting to

dx.doi.org/10.1021/jp2073123 |*J. Phys. Chem. A* 2012, 116, 536–545

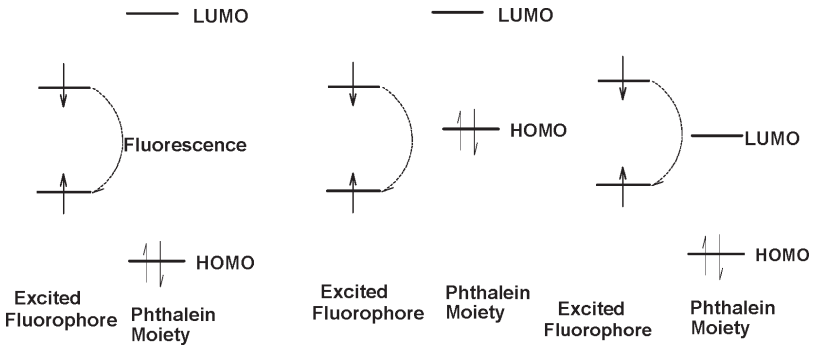

Figure 6. Molecular orbital diagram and electron transfer mechanism in the excited state.

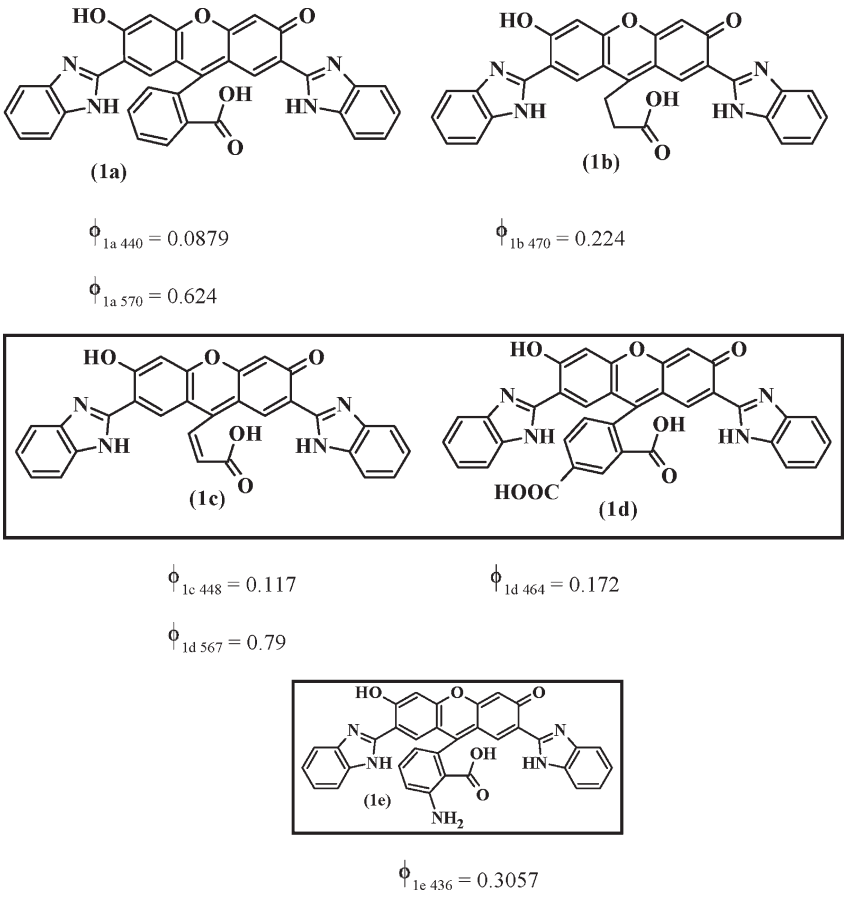

Figure 7. Structure and fluorescence quantum efficiency at different wavelength of fluorescein derivatives.

observe that this red-shifted excitation is not a function of pH (Table 1, Figure 1). Compound **1a** contains three phenyl rings having conjugation. Dual emissions of dye **1a** arising out of excitation at 303 nm are located in the region 408−432 nm along with a long wavelength emission at 570 nm (Table 1, Figure 2). In the case of **1b**, there are only two phenyl rings on the central carbon atom and weakly conjugated two carbon atoms as against the fully conjugated additional aromatic ring in **1a**. Both of the phenyl rings carry a benzimidazole moiety. Dual emission phenomena are not found to be promising for the dyes **1b** and **1c**. In the case of **1b**, there is no additional conjugated phenyl ring to central carbon atom of phthalein ring, and it has weakly conjugated two carbon atoms. The compound **1b** on excitation at 300 nm has emission in the region 412−440 nm (Table 1; Figures 3 and 4, Supporting Information). The additional conjugation is totally absent in the dye **1c**, and it has an excitation in the region 294−318 nm with a blue-shifted emission band from 426 to 462 nm (Table 1; Figures 5 and 6, Supporting Information). In the case of dye **1d**, which carries an electron withdrawing carboxyl substituent at the para position, the usual excitation at 495 nm was found to be absent at pH 12 and 13. However, an additional excitation at 545 nm was located (Table 1; Figure 7, Supporting Information). Dye **1d** showed a strong emission band at the longer wavelength 572 nm and comparatively weak emission band at 435 nm on excitation at near 300 nm (Table 1; Figure 8, Supporting Information).

dx.doi.org/10.1021/jp2073123 |*J. Phys. Chem. A* 2012, 116, 536–545

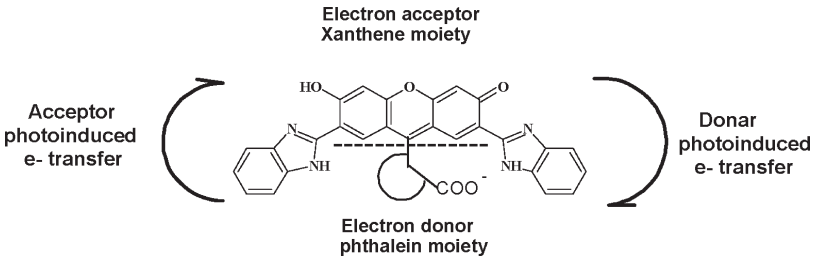

Figure 8. Fluorescein derivative divided into two parts: one electron donor phthalein moiety and electron acceptor xanthene (2,7-bis(1*H*-benzimidazol-2-yl)-6-hydroxy-3*H*-xanthen-3-one) moiety.

Dye **1e** contains an electron releasing amino substituent. For dye **1e**, an excitation band at 300 nm was observed along with a weak excitation band located at 540 nm (Table 1; Figure 9, Supporting Information). Dye **1e** showed emission in the region 411−443 nm on excitation at 300 nm (Table 1; Figure 10, Supporting Information). Dual emission phenomenon was not found in **1e**.

Effect of pH on Photophysical Properties. At pH 6, dye **1a** has three absorptions located at 303, 495, and 543 nm. The absorption at 432 nm experiences a red shift beyond pH 6. At pH values 7, 8, and 9, this red-shifted absorption band appears at 495 nm, while the other two absorptions at 303 nm and 543 nm remain unchanged over the entire pH range. Upon raising the pH above 9, the middle absorption band, which experienced a red shift from 432 to 495 nm, disappeared completely (Table 1, Figure 1). At all pH, the excitation at 303 nm was accompanied by dual emission (Table 1, Figure 2), while another two absorptions did not show any accompanying emissions. The short wavelength emission located at around 408 nm (at pH 6) experienced a red shift up to pH 9; the red-shifted emission appeared at 434 nm. Beyond pH 9, the emission maxima returned to the original value around 410 nm. The long wavelength emission remained constant through the entire pH range and was located at around 570 nm (Table 1, Figure 2). The dye **1b**, which is devoid of a phenyl group at the central carbon atom, had a different behavior. At pH values up to 9 only one absorption centering at 300 nm was observed. Beyond pH 9, additional absorption peaks appeared (Table 1; Figure 3, Supporting Information). The excitation at 300 nm was accompanied by a single emission at 436 nm (at pH 6), and it experienced a red shift until the pH value was 9; the blue-shifted emission appeared at 430−440 nm. From pH 10 onward, the same excitation gave dual emission as shown in Table 1. The dual emission ceased to exist at higher alkalinity, i.e., at pH 12 and pH 13 (Table 1; Figure 4, Supporting Information). In the case of dye **1c** where the central carbon atom is conjugated to an aliphatic residue, there was no dual emission at any pH value. The short wavelength excitation at around 300 nm had a single emission located at 460 nm, which experienced a blue shift from pH 11 onward (Table 1; Figures 5 and 6, Supporting Information). The dye **1d** behaved in a similar way to **1a** except the fact that dual emission arising out of short wavelength excitation was not sensitive to pH (Table 1; Figure 7, Supporting Information). The short wavelength excitation was located at 300 nm. An absorption located at 495 nm up to pH 11 disappeared beyond pH 11. Long wavelength absorption started appearing at 545 nm from pH 9 onward (Table 1; Figure 8, Supporting Information). For **1e**, an excitation band near 300 was located for all pH values (except for pH 12 was located at 285 nm), and a long wavelength excitation band for all pH values were located at 540 nm (except pH 12 was located at 490 nm, and

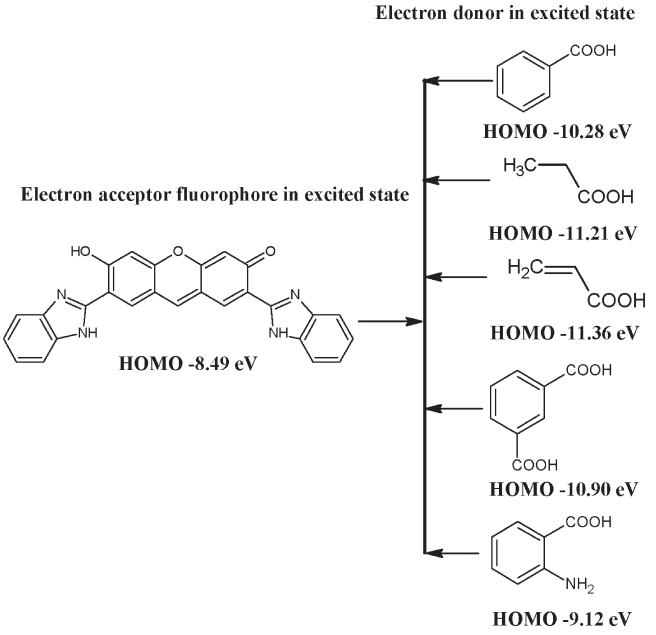

Figure 9. HOMO energy of 2,7-bis(1*H*-benzimidazol-2-yl)-6-hydroxy-3*H*-xanthen-3-one as the electron acceptor (fluorophore) and the phthalein moiety (electron donor).

For pH 8, at 490 nm an excitation band along with 535 nm was located). The dye **1e** showed photophysical properties similar to **1c** except the fact that it showed dual emission at pH 11 (Table 1; Figures 9 and 10, Supporting Information). Fluorescein has a single emission at 520 nm. Incorporation of ESIPT in fluorescein causes dual emission. ESIPT molecules exist in two forms (keto and enol) at the first excited state. The existence of two forms causes dual emission in compounds **1a** and **1d**; short wavelength emission appears to be due to the enol form, and long wavelength emission appears to be due to the keto form. After incorporation of the ESIPT hydroxy benzimidazole moiety in fluorescein, the longer emission experiences a red shift, and the emission occurs at 570 nm.

2-(2′,4′-Dihydroxy phenyl) benzimidazole **3** absorbs at 326 nm and has dual emission at 374 and 444 nm (Figure 11, Supporting Information) After incorporation in to the fluorescein system, **1a** shows dual emission at 434 and 570 nm and **1d** at 435 and 572 nm. **1b**, **1c**, and **1e** shows single emission at 440, 462, and 430 nm, respectively; these results clearly indicate that the fluorescein moiety is responsible for the red shift of the longer wavelength emission of **3**.

The change in emission intensity with respect to pH values for each emission wavelength irrespective of its emission band are

dx.doi.org/10.1021/jp2073123 |*J. Phys. Chem. A* 2012, 116, 536–545

Table 2. Physical Properties and Relative Fluorescence Quantum Yields of Compounds 1a−1e

compd	mol wt	thermal stability (°C (%))	quantum yield at short wavelength	quantum yield at long wavelength	total quantum yield
1a	564.54	323(81.17)	$\phi_{1a\ 440}$ = 0.0879	$\phi_{1a\ 570}$ = 0.624	0.7119
1b	514.48	300(81.38)	$\phi_{1b\ 470}$ = 0.224		0.224
1c	516.50	244(77.81)	$\phi_{1c\ 448}$ = 0.117		0.117
1d	608.55	335(72.84)	$\phi_{1d\ 464}$ = 0.172	$\phi_{1d\ 567}$ = 0.79	0.962
1e	579.56	314(78.40)	$\phi_{1e\ 436}$ = 0.3057		0.3057

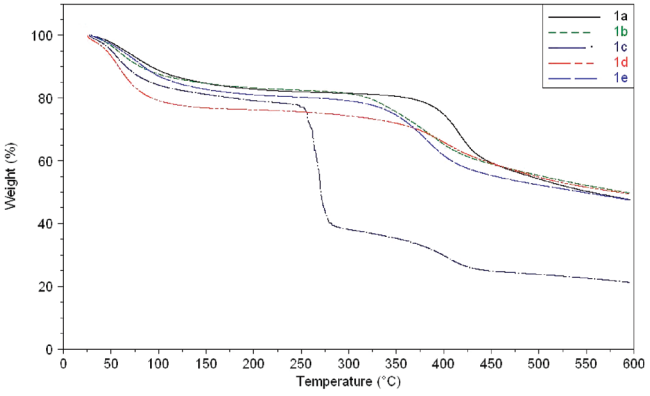

Figure 10. Thermo gravimetric analysis overlay graph of dyes **1a**−**1e**.

presented in Figures 3 and 4. The fluorescence intensity ratio of the short emission band to the long emission band vs pH curves for fluorescein derivatives **1a** and **1d** in aqueous solution are given in Figure 5. It was observed that for compound **1a** and **1d**, an exact opposite behavior of the ratiometric response was located with respect to the change in pH value.

Fluorescence Properties of Fluorescein-Derivatives. Fluorescent properties of fluorescein-derivatives are observed to be truly controlled by the rate of photoinduced electron transfer from the phthalein moiety (electron donor) to the singlet excited state of the xanthene moiety (electron acceptor fluorophore) in the excited state. The fluorescence properties of fluorescein are highly dependable on oxidation potential and reduction potential of the phthalein moiety. The electron density on the phthalein ring influences the oxidation potential and reduction potential, which finely controlled the fluorescence properties of substituted fluorescein.[50,51] An example is well explained in the literature.[52] The presence of electron-withdrawing groups on the phthalein moiety lowers the electron density controlling the fluorescence quantum efficiency of fluorescein derivatives.[53,54]

It is known that dicarboxyfluorescein is highly fluorescent (ϕ_{fl} = 0.817), while disubstituted trimethyl ester is weakly fluorescent (ϕ_{fl} = 0.001). A similar phenomenon has also been observed in the 6-carboxyfluorescein derivative (ϕ_{fl} = 0.869).[53] Fluorescence quantum efficiency of fluorescent compounds is also attributed to the energy values of HOMO and LUMO (Figure 6).

The dyes **1b**, **1c**, and **1e** showed a single emission band, while **1a** and **1d** showed two emission bands. In the case of dual-emitting dyes, the relative fluorescence quantum efficiencies at each emission wavelengths were calculated by using anthracene and fluorescein as standards(Figure 7).[55,56] In the case of the amino substituted derivative **1e**, fluorescence quantum efficiency for short wavelength emission was observed to be higher (ϕ_{1e436} = 0.3057); the oxidation potential of the phthalein moiety was also higher,[50,51] and the energy of HOMO was −9.12 eV. Fluorescence quantum efficiency at long wavelength emission was found to be higher for carboxylic acid substituted fluorescein **1d** (ϕ_{1d567} = 0.79); increased reduction potential of the phthalein moiety was observed,[50,51] and the energy of HOMO was −10.90 eV.

The photophysical properties of fluorescein derivatives are usually understood by differentiating the molecule into two parts: xanthene and phthalein (Figure 8). Energy values of HOMO are independently represented in Figure 9. Our observation suggests that the HOMO energy level of the phthalein moiety decides whether electron transfer to the excited xanthene ring occurs. It can be seen that low HOMO energy of the phthalein moiety gives rise to high fluorescence. The HOMO and LUMO energy levels of benzoic acid, propionic acid, acrylic acid, 1,3-dibenzoic acid, and 2-aminobenzoic acid were estimated by computational semiempirical (AM1) calculations.

Relative Fluorescence Quantum Yield. Quantum yields of compounds **1a**−**1e** were determined by the comparative method using known standards (fluorescein and anthracene) and formula 1.[55,56] The quantum efficiency of compound **1a** was found to be 0.0879 at short wavelength and 0.624 at long wavelength. For dye **1b** and **1c**, the quantum efficiency was found to be 0.224 and 0.117, respectively. For compound **1d**, the quantum efficiency was found to be 0.172 and 0.79, respectively, for short and long wavelength emissions. For compound **1e**, the quantum efficiency was found to be 0.305. Relative fluorescence quantum yields are summarized for compounds **1a**−**1e** in Table 2.

$$\phi_X = \phi_{ST}(\mathrm{Grad}_X/\mathrm{Grad}_{ST})(\eta_X{}^2/\eta_{ST}{}^2) \quad (1)$$

where ϕ_X = quantum yield of unknown sample; ϕ_{ST} = quantum yield of standard used; Grad_X = gradient of unknown sample; Grad_X = gradient of standard used; $\eta_{ST}{}^2$ = refractive index of solvent for standard sample; and $\eta_X{}^2$ = refractive index of solvent for unknown sample.

Thermal Stability of Dyes. In order to give more insight into the dyes **1a**−**1e**, the thermal studies of the compounds have been carried out using thermal gravimetric techniques (TGA). The thermogravimetric studies have been carried out in the temperature range 50−600 °C under nitrogen gas at a heating rate of 10 °C min^{-1}. The TGA results indicated that the synthesized dyes are stable up to 300 °C. TGA revealed the onset decomposition temperature (T_d) of dyes **1a**−**1e** at 323, 300, 244, 335, and 314 °C, respectively. Above 300 °C, the thermo gravimetric curve of the synthesized compounds show a major loss in weight. The comparisons of the T_d show that the thermal stability of **1a**−**1e** decreases in the order **1d** > **1a** > **1e** > **1b** > **1c**. The results showed that synthesized dyes have good thermal stability, except dye **1c**, which showed a sharp decomposition point at 244 °C and completely decomposed beyond 450 °C. However, dyes **1a**, **1b**, **1d**, and **1e** showed elongated decomposition behaviors and

dx.doi.org/10.1021/jp2073123 |J. Phys. Chem. A 2012, 116, 536–545

completely decomposed beyond 600 °C as shown in Figure 10 and Table 2.

4. CONCLUSIONS

Herein, we have introduced new fluorescent molecules with emphasis on its photophysics of pH sensitivity. It may find potential application in simultaneous analytical assay development and measurement of intracellular pH while scanning the biologically active species for its immunoassay. Implementation of two band ratiometry sensing of dual emitting fluorescent probe molecules such as **1a** and **1d** would be highly useful during the expansion of an immunoassay. Supplementarily, fluorescent properties for a new series of fluorescein compounds were discussed by reasonable principle from the HOMO energy and fluorescence quantum efficiency. This rational relationship gives useful protocol for design and synthesis of a new kind of fluorescent compounds from the application point of view.

■ ASSOCIATED CONTENT

Supporting Information. Preparation, analysis, graph, and table for absorption-emission versus pH; and values and figures for HOMO and LUMO orbitals of each molecule. This material is available free of charge via the Internet at http://pubs.acs.org.

■ AUTHOR INFORMATION

Corresponding Author

* E-mail: n.sekar@ictmumbai.edu.in or nethi.sekar@igmail.com.

■ ACKNOWLEDGMENT

We are greatly thankful to IIT Mumbai for recording the ^{1}H NMR, ^{13}C NMR, and mass spectra.

■ REFERENCES

(1) Vicentini, L. M.; Villereal, M. L. *Life Sci.* **1986**, *38*, 2269–2276.
(2) Kubohara, Y.; Okamoto, K. *FASEB J.* **1991**, *8*, 869–874.
(3) Ronnie, M. A.; Kjell, C.; Anders, L.; Hjalmar, B. *Anal. Biochem.* **2000**, *283*, 104–110.
(4) Charier, S.; Ruel, O.; Baudin, J.-B.; Alcor, D.; Allemand, J.-F.; Meglio, A.; Jullien, L. *Angew. Chem., Int. Ed.* **2004**, *43*, 4785–4788.
(5) Wong, L. S.; Birembaut, F.; Bocklesby, W. S.; Frey, J. G.; Bradley, M. *Anal. Chem.* **2005**, *77*, 2247–2251.
(6) Cho, J. K.; Wong, L. S.; Dean, T. W.; Ichihara, O.; Muller, C.; Bradley, M. *Chem. Commun.* **2004**, 1470–1471.
(7) Cho, J. K.; White, P. D.; Klute, W.; Dean, T. W.; Bradley, M. *J. Comb. Chem.* **2003**, *5*, 632–636.
(8) Wong, L. S.; Brocklesby, W. S.; Bradley, M. *Sens. Actuators B* **2005**, *107*, 957–962.
(9) Bradley, M.; Alexander, L.; Duncan, K.; Chennaoui, M.; Jones, A. C.; Sanchez-Martin, R. M. *Bioorg. Med. Chem. Lett.* **2008**, *18*, 313–317.
(10) Vasylevska, A. S.; Karasyov, A. A.; Borisov, S. M.; Krause, C. *Anal. Bioanal. Chem.* **2007**, *387*, 2131–2141.
(11) Lavis, L. D.; Rutkoski, T. J.; Raines, R. T. *Anal. Chem.* **2007**, *79*, 6775–6782.
(12) Smith, J. P.; Drewes, L. R. J. *Biol. Chem.* **2006**, *281*, 2053–2060.
(13) Barnard, S. M.; Walt, D. R. *Nature* **1991**, *353*, 338–340.
(14) Bronk, K. S.; Michael, K. L.; Pantano, P.; Walt, D. R. *Anal. Chem.* **1995**, *67*, 2750–2754.
(15) Grynkiewicz, G.; Poenie, M.; Tsien, R. Y. *J. Biol. Chem.* **1985**, *260*, 3440–3450.
(16) Bright, G. R.; Fisher, G. W.; Rogowska, J.; Taylor, D. L. *Methods Cell Biol.* **1989**, *30*, 157–192.
(17) O'Connor, N.; Silver, R. B. *Methods Cell Biol.* **2007**, *81*, 415–433.
(18) Douhal, A.; Amat-Guerri, F.; Acuna, A. *J. Phys. Chem.* **1995**, *99*, 76–80.
(19) English, D.; Zhang, W.; Kraus, G.; Petrish, J. *J. Am. Chem. Soc.* **1997**, *119*, 2980–2986.
(20) Tian, Y.; Chen, C. Y.; Yang, C. C.; Young, A. C.; Jang, S. H.; Chen, W. C.; Jen, A. K. Y. *Chem. Mater.* **2008**, *20*, 1977–1987.
(21) Pang, Y.; Chen, W. Excited-State Intramolecular Proton Transfer in 2-(2′-Hydroxyphenyl)benzoxazole Derivatives. In *Hydrogen Bonding and Transfer in the Excited State*; Han, K. L., Zhao, G. J, Eds.; John Wiley & Sons: New York, 2011; Vols. I and II, pp 747−760.
(22) Chen, W.; Pang, Y. *Tetrahedron Lett.* **2010**, *51*, 1914–1918.
(23) Padalkar, V.; Tathe, A.; Gupta, V.; Patil, V.; Phatangare, K.; Sekar, N. *J. Fluoresc.* **2011**. DOI: 10.1007/s10895-011-0962-8.
(24) Dandan, Y.; Zhao, S.; Guo, J.; Zhang, Z.; Zhang, H.; Liu, Y.; Wang, Y. *J. Mater. Chem.* **2011**, *21*, 3568–3570.
(25) Pang, Y.; Xu, Y. *Dalton Trans.* **2011**, *40*, 1503–1509.
(26) Douhal, A.; Amat-Guerri, F.; Acuna, A. *Angew. Chem., Int. Ed.* **1997**, *36*, 1514–1516.
(27) Woolf, G.; Meizig, M.; Schneider, S.; Dorr, F. *Chem. Phys.* **1983**, *77* (2), 113–221.
(28) Abou-Zied, O.; Jimenezm, R.; Thompson, E.; Miller, D.; Romseberg, F. *J. Phys. Chem. A* **2002**, *106*, 3665–3672.
(29) Huang, J.; Peng, A.; Fu, H.; Ma, Y.; Zhai, T.; Yao, J. *J. Phys. Chem. A* **2006**, *110*, 9079–9083.
(30) Cheng, Y. M.; Pu, S. C.; Hsu, C. J.; Lai, C. H.; Pi, T. *Chem. Phys. Chem.* **2006**, *7*, 1372–1381.
(31) Jangwon, S.; Kim, S.; Park, S.; Soo, Y. *Bull. Korean Chem. Soc.* **2005**, *26*, 1706–1710.
(32) Vazquez, S. R.; Rodriguez, M. C. R.; Mosquera, M. *J. Phys. Chem. A* **2008**, *112*, 376–387.
(33) Ghiggino, K.; Scully, A.; Leaver, I. *J. Phys. Chem.* **1986**, *90*, 5089–5093.
(34) Kelly, R.; Schulman, S.; Schulman, S. Molecular Luminescence Spectroscopy, Methods and Applications, Part 2; Wiley Interscience: New York, 1988; Chapter 6.
(35) Ghiggino, K.; Scully, A.; leaver, I. *J. Phys. Chem.* **1986**, *90*, 5089–5093.
(36) Kosower, E.; Huppert, D. *Annu. Rev. Phys. Chem.* **1986**, *37*, 127–156.
(37) Law, K.; Shoham, J. *J. Phys. Chem.* **1995**, *99*, 12103–12108.
(38) Goodman, J.; Brus, L. *J. Am. Chem. Soc.* **1978**, *100*, 7472–7474.
(39) Here, J.; Pedersen, S.; Banares, L.; Zewali., A. *J. Chem. Phys.* **1992**, *97*, 9046–9062.
(40) Formosinho, S.; Arnaut, J. *J. Photochem. Photobiol., A* **1993**, *75*, 21–48.
(41) Segala, M.; Dorirngues, N.; Livotto, V.; Stefani, V. *J. Chem. Soc., Perkin Trans. 2* **1999**, *2* (6), 1123–1127.
(42) Elouera, J.; Katriezky, A.; Denisko, O. *Adv. Heterocycl. Chem.* **2000**, *76*, 1–84.
(43) Arnaut, L.; Formosinho, S. *J. Photochem. Photobiol., A* **1993**, *75*, 1–20.
(44) Formosinho, S.; Arnaut, L. *J. Photochem. Photobiol., A* **1993**, *75*, 21–48.
(45) Rios, N.; Rios, M. *J. Phys. Chem. A* **1998**, *102* (9), 1560–1567.
(46) Vollmer, F.; Rettig, W.; Birckner, E. *J. Fluoresc.* **1994**, *4* (1), 65–69.
(47) Minkin, V.; Garnovski, A.; Elguero, J.; Katriezky, A.; Denisko, O. *Adv. Heterocycl. Chem.* **2000**, *76*, 157–323.
(48) Doroshenko, A.; Posokhov, E.; Verezubova, A.; Ptyagina, L. *J. Phys. Org. Chem.* **2000**, *13* (5), 253–265.
(49) Kiyoshi, T.; Tsutomu, K.; Hiroko, A.; Makoto, D.; Satoru, I. *J. Org. Chem.* **2001**, *66*, 7328–7333.
(50) Kumi, T.; Tetsuo, M.; Naoki, U.; Yasuteru, U.; Kazuya, K.; Tsunehiko, H.; Tetsuo, N. *J. Am. Chem. Soc.* **2001**, *123*, 2530–2536.
(51) Tetsuo, M.; Yasuteru, U.; Kumi, T.; Tetsuo, N.; Kei, O.; Shunichi, F. *J. Am. Chem. Soc.* **2003**, *125*, 8666–8671.

(52) Tanaka, K.; Miura, T.; Umezawa, N.; Urano, Y.; Kikuchi, K.; Higuchi, T.; Nagano, T. *J. Am. Chem. Soc.* **2001**, *123*, 2530–2536.
(53) Miura, T.; Urano, Y.; Tanaka, K.; Nagano, T.; Ohkubo, K.; Fukuzumi, S. *J. Am. Chem. Soc.* **2003**, *125*, 8666–8671.
(54) Tasuku, U.; Yasuteru, U.; Ken-ichi, S.; Hideo, T.; Hirotatsu, K.; Kazuya, K.; Kei, O.; Shunichi, F.; Tetsuo, N. *J. Am. Chem. Soc.* **2004**, *126*, 14079–14085.
(55) Williams, A.; Winfield, S.; Miller, J. *Analyst* **1983**, *108*, 1067–1071.
(56) Dhami, S.; De Mello, A. J.; Rumbles, G.; Bishop, S. M.; Phillips, D.; Beeby, A. *Photochem. Photobiol.* **1995**, *61*, 341–346.